Korean J. Chem. Eng., **29**(11), 1577-1584 (2012)
DOI: 10.1007/s11814-012-0058-4

A comprehensive study on wastewater treatment using photo-impinging streams reactor: Continuous treatment

Sayed Javid Royaee*,, Morteza Sohrabi**,†, and Narges Fallah****

*Refining Technology Development Division, Research Institute of Petroleum Industry, Tehran, Iran
**Chemical Engineering Department, Amirkabir University of Technology, Tehran, Iran
(*Received 12 February 2012 • accepted 27 April 2012*)

Abstract−The degradation of phenol was investigated in a continuous flow impinging streams system. In the first step, statistical experimental designs were used to optimize the process of phenol degradation in a photo-impinging streams reactor. The more important factors affecting phenol degradation ($p<0.05$) were screened by a two-level Plackett-Burman design. Four of the latter parameters, namely phenol concentration, catalyst loading, pH and slurry flow rate, were selected for final process optimization, applying central composite design (CCD). The predicted data showed that the maximum removal efficiency of phenol (99%) could be obtained under the optimum operating conditions (phenol concentration=50 mg l^{-1}, catalyst loading=2.1 g l^{-1}, pH 6.2 and slurry flow rate=550 ml min^{-1}). These predicted values were then verified by certain validating experiments. A good correlation was observed between the predicted data and those determined by the experimental study. This may confirm the validity of the statistical optimum strategy. Finally, continuous degradation of phenol was performed, and the results indicated a higher efficiency and an increased performance capability of the present reactor in comparison with the conventional processes.

Key words: Phenol Degradation, Plackett-Burman Design, Central Composite Design, Photo-impinging Streams Reactor-Continuous Flow

INTRODUCTION

Hazardous organic compounds are one of the major causes of environmental pollution, particularly in water resources. The heterogeneous photocatalytic decomposition of these compounds using TiO_2 semiconductor materials as photocatalysts has often been successfully applied in the treatment of contaminated water and air streams [1-6]. However, there are two essential issues on photocatalytic processes: photon transfer limitations and mass transfer limitations [7]. Recently, Royaee et al. [8,9] introduced a new photoreactor by which such limitations could be eliminated. An inherent disadvantage of batch reactors is the separation of catalyst after the treatment. However, this phenomenon can be prevented by implementing a continuous treatment of wastewater in a reactor [10].

Statistical experimental designs such as Plackett-Burman and response surface methodology (RSM) [11,12] can collectively optimize all the affecting parameters to eliminate the limitations of a single-factor optimization process. Plackett-Burman design provides a fast and effective way to identify the important factors among a large number of variables, thereby saving time and maintaining convincing information on each parameter [13]. RSM, which includes factorial design and regression analysis, helps in evaluating the important factors, building models to study the interactions between the variables, and selecting the optimum conditions of variables or desirable responses [14].

In the present study, degradation of phenol has been investigated in a continuous flow impinging streams system. An experimental design analysis was first employed in order to determine and optimize the significant factors affecting phenol degradation.

†To whom correspondence should be addressed.
E-mail: sohrabi@aut.ac.ir

EXPERIMENTAL

1. Materials

Titanium dioxide nanoparticle (P25) was supplied by Degussa, Germany. Phenol with above 99.5% purity, phenol test kits, NaOH and H_2SO_4 were all obtained from Merck Co.

2. Analytical Procedure

The concentration of phenol was measured by a UV-visible spectrophotometer (Dr 2800 Hach Co.) at a wavelength of 495 nm using the 4-aminoantipyrine method. Owing to the presence of TiO_2 powders in the system, the samples were first filtered using a 0.22 μm syringe filter (Millipore) to remove particles.

3. Photo-reactor

In the first step, batch circulation photocatalysis experiments were performed to determine the optimum operating conditions. A schematic diagram of the photo-impinging streams reactor used in this study is shown in Fig. 1(a). The apparatus consisted of a cylindrical vessel made of quartz and equipped with 16 low-pressure mercury vapor lamps, with a dominant emission line at 253.7 nm (TUV 8W from Philips Co.) as irradiation sources. Two pressure nozzles were mounted on the same axis in front of each other spraying two jets of slurry.

A stream of air with a specified flow rate was continuously supplied to the slurry solution. To prevent hole/electron formation, prior to turning on the illumination the catalyst was placed in the feed reservoir at dark. The phenol solution was then added and the suspension was saturated with air while being stirred with a magnetic

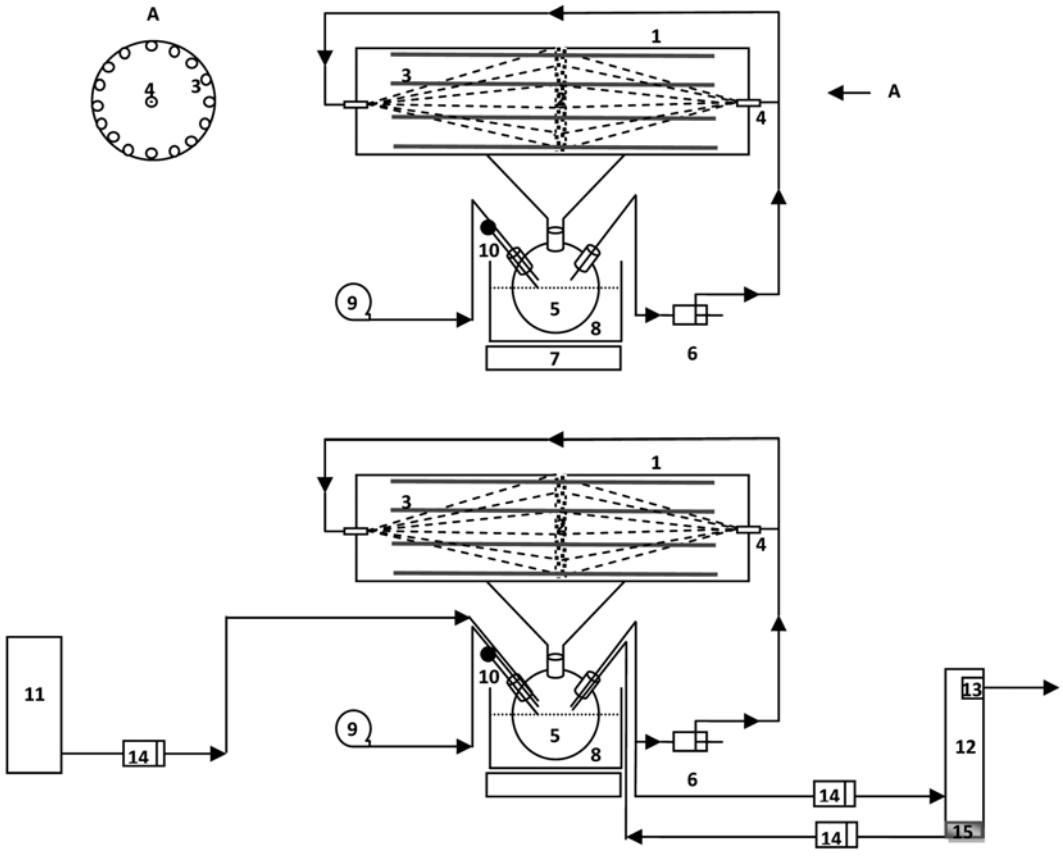

Fig. 1. Schematic diagram of the photo-reactor.

(a) Batch mode.

1. Reaction vessel 3. UV lamps 5. Feed reservoir 7. Magnetic mixer 9. Air pump
2. Impingement zone 4. Feed nozzle 6. Gear pump 8. Cooling system 10. pH sensor

(b) Continuous mode.

11. Phenol solution tank 12. TiO_2 settler 13. Filter 14. Peristaltic pumps 15. Separated photocatalyst

stirrer in darkness for 30 min to establish the adsorption-desorption equilibrium. The gear pump was then switched on and the suspension, after passing through the two nozzles, was irradiated with UV light and collided in the impingement zone. Samples were regularly withdrawn from the reactor and filtered to remove all the suspended solid particles prior to analysis. The pH of the solution was adjusted by addition of 0.1 mol l^{-1} NaOH or H_2SO_4 as required and monitoring with a digital pH meter. The temperature of the photo reactor was maintained unchanged by a water jacket constructed around the feed reservoir. The suspension was kept uniform in composition by agitation with a magnetic stirrer.

Further studies were carried out on continuous flow photocatalytic treatment of phenol. In such studies, the TiO_2 particles were added to the phenol solution in the feed tank with continuous stirring. The slurry was then conducted from the feed tank to the reaction vessel via a peristaltic pump. The treated effluent flowed out of the reactor to a separator/settler with a flow rate equal to that of the feed, and was then passed through a filter. Separated photocatalyst may be recycled to the feed tank. Samples were regularly withdrawn from the filter outlet. Fig. 1(b). demonstrates such an operation.

4. Experimental Designs

4-1. Plackett-burman Design

In the first step, Plackett-Burman design [15] was used to screen the most significant factors from among a large number of variables that might influence the performance of the photocatalytic process. In this study, a 12-run Plackett-Burman design was applied to evaluate eleven factors (including one dummy variable). In this order, two levels were selected for each factor to run the tests. The coded high and low levels were set as +1 and −1, respectively, as listed in

Table 1. Levels of the variables in Plackett-Burman design

Variables	Symbol	Experimental value	
		Low (−1)	High (+1)
Calcination temp. (°C)	A	0	500
Catalyst loading (g L^{-1})	B	0.5	2
pH	C	4	9
Air flow rate (L min^{-1})	D	0.2	2
PheOH concentration (mg L^{-1})	E	50	100
Temperature (°C)	F	25	55
Number of lamp	G	8	16
CH2O2/CPhOH	H	0	50
CS2O82-/CPhOH	I	0	10
Slurry flow rate (ml min^{-1})	J	250	450
Dummy	K	0	0

Table 2. Plackett-Burman design of variables (in coded levels) and phenol degradation after 30 min as response

Std. order	Run order	Experimental value											Phenol degradation (%)
		A	B	C	D	E	F	G	H	I	J	K	
9	1	−1	−1	−1	+1	+1	+1	−1	+1	+1	−1	+1	61.11
11	2	−1	+1	−1	−1	−1	+1	+1	+1	−1	+1	−1	94.15
6	3	+1	+1	+1	−1	+1	+1	−1	+1	−1	−1	+1	36.67
10	4	+1	−1	−1	−1	+1	+1	+1	−1	+1	+1	+1	73.25
8	5	−1	−1	+1	+1	+1	−1	+1	+1	−1	+1	−1	59.47
12	6	−1	−1	−1	−1	−1	−1	−1	−1	−1	−1	−1	29.01
2	7	+1	+1	−1	+1	−1	−1	−1	+1	+1	+1	−1	87.47
3	8	−1	+1	+1	−1	+1	−1	−1	−1	+1	+1	+1	43.91
7	9	−1	+1	+1	+1	−1	+1	+1	−1	+1	−1	−1	61.25
5	10	+1	+1	−1	+1	+1	−1	+1	−1	−1	+1	+1	57.45
4	11	+1	−1	+1	+1	−1	+1	−1	−1	−1	+1	+1	26.13
1	12	+1	−1	+1	−1	−1	−1	+1	+1	+1	−1	−1	68.55

Table 1. The values of the two levels were set according to the previous preliminary experimental results performed by the present authors [9]. The Plackett-Burman design and the response value of phenol degradation (percent of phenol removed after 30 min) are shown in Table 2. It is important to note that the order of the experimental runs was randomized to get meaningful statistical results. Experimental procedures were identical for all runs except for the variable factors as shown in Table 2.

4-2. Central Composite Design

To determine the optimum conditions for degradation, the crucial factors were screened and the central composite design (CCD) was applied to establish the optimal levels of the signiant factors and the interactions of such variables on phenol degradation. A four-factor, five-level CCD with 30 runs was employed. Tested variables (phenol concentration, catalyst loading, pH and flow rate) were denoted as X_1, X_2, X_3, and X_4, respectively. Each of these variables was assessed at five different levels, combining factorial points (−1, +1), axial points (−2, +2), and central point (0), as shown in Table 3.

The principle of response surface methodology (RSM) has been described by Khuri and Cornell [16] and its objective is to optimize the response based on factors investigated [17]. An empirical second-order polynomial model for independent variables was considered as follows:

$$Y = b_0 + \sum_{i=1}^{k} b_i X_i + \sum_{i=1}^{k-1} \sum_{j=2}^{k} b_{ij} X_i X_j + \sum_{i=1}^{k} b_{ii} X_i^2 + e \quad (1)$$

where, Y, is the predicted response (phenol degradation) X_i and X_j, are input variables that influence the response Y, b_0, is the offset term, bi, is the linear effect, b_{ij}, is the squared effect, b_{ii}, is the interaction effect and k, is the number of variables.

Analysis of variance (ANOVA) was conducted to determine the significance of model and regression coefficients. The quality of the polynomial equation was judged by the determination of coefficient (R^2), and its statistical significancewas checked by Fischer's F-test. The significance of regression coefficients was tested by Student's t-test. The response surface and contour plots of the model-predicted responses were utilized to assess the interactive relationships between the significant variables. Design-Expert Version 7.1.3 (Stat-Ease Inc., Minneapolis, USA) was used to design experiments and to analyze the regression and graphical experimental data obtained.

Table 3. Levels of the variables in the CCD

Variable	Symbol	Coded levels				
		−2	−1	0	+1	+2
PheOH concentration (mg L^{-1})	X1	25	50	75	100	125
Catalyst loading (g L^{-1})	X2	0.05	0.7	1.35	2	2.65
pH	X3	1	3	5	7	9
Slurry flow rate (ml min^{-1})	X4	300	400	500	600	700

RESULTS AND DISCUSSION

As mentioned earlier, Plackett-Burman design and RSM have been successfully employed to optimize conditions for photocata-

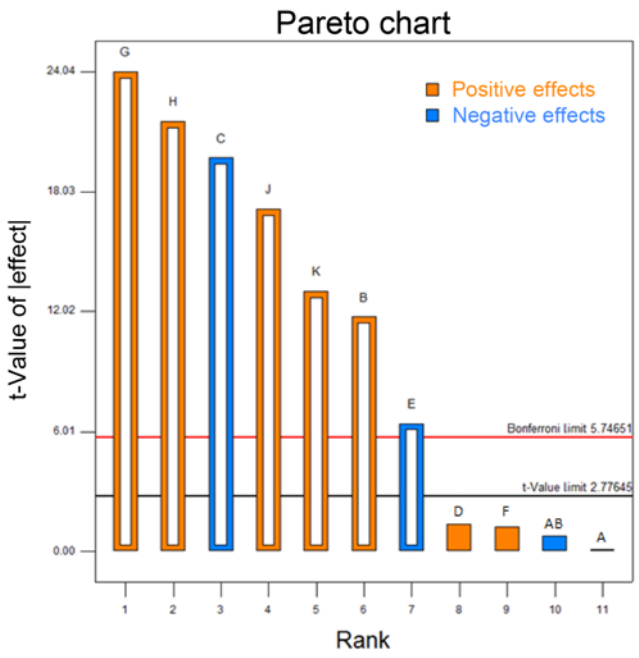

Fig. 2. Rank of factors.

Table 4. Results of analysis of variance for Plackett-Burman design

Source	Sum of squares	df	Mean square	F value	p-value Prob>F
Model	0.50	10	0.050	346.80	0.0418
A	3.203E-006	1	3.203E-006	0.022	0.9063
B	0.033	1	0.033	229.91	0.0419
C	0.094	1	0.094	648.66	0.0250
D	4.490E-004	1	4.490E-004	3.08	0.3296
E	0.010	1	0.010	68.91	0.0463
F	3.741E-004	1	3.741E-004	2.57	0.3551
G	0.14	1	0.14	964.56	0.0205
H	0.11	1	0.11	775.72	0.0228
I	0.072	1	0.072	491.40	0.0287
J	0.041	1	0.041	283.17	0.0378
Residual	1.456E-004	1	1.456E-004		
Cor total	0.51	11			

lytic phenol degradation in a Photo-Impinging streams reactor. The results are presented here.

1. Screening of Important Variables

The data listed in Table 2 demonstrate a wide range of phenol degradation (from 26.13 to 94.15%) in 12 trials. This observation necessitates the optimization of phenol degradation process conditions in order to achieve a high efficiency. Analysis of the t-values of 10 factors (Fig. 2) showed that A, B, D, F, G, H, I and J had positive effects on phenol degradation, whereas C and E had negative effects. Rank of these effects is shown in Fig. 2. Table 4 presents the results of variance analysis. A variable having confidence level of above 95% is considered a significant parameter. Thus, variables B, C, E, G, H, I and J are the significant factors, while variables A, D and F with confidence levels below 95%, are supposed to be insignificant. As increase in light intensity promotes the degradation efficiency [9] the effect of such a parameter was first tested in five levels. In contrast to light intensity, the co-oxidants are not essential for photocatalytic process and as such were not considered in optimization studies.

2. Effect of Light Intensity

Photocatalytic reaction rate depends largely on the radiation absorption of the photocatalyst. Ollis et al. [18] published a review on the effect of light intensity upon the rate of photocatalytic processes and concluded that at low light intensities (0-20 mW/cm^2), the rate increases linearly with increasing light intensity (first order). However, beyond a certain value (approximately 25 mW/cm^2), the rate becomes dependent upon the square root of the light intensity (half order), while at higher light intensities the rate would level off to become independent of the light intensity. This may be acceptable since at low light intensity, reactions involving electron-hole formation are predominant and electron-hole recombination is negligible. However, at increased light intensity, electron-hole pair separation competes with recombination, thereby imposing lower effect on the reaction rate.

To study the influence of light intensity on the photocatalytic degradation of phenol, the photo reactor was equipped with 16 low-pressure mercury vapor lamps. A number of experiments were carried out, applying various light intensities generated from 2, 4, 6, 8 and 16 lamps, respectively. Radiation intensities were determined by ferrioxalate actinometry and are here presented as fractions of the initial photonic flow (ϕ/ϕ_0) that is considered for eight lamps. Within the range of intensities studied, the initial rates were observed to vary linearly with the photonic flow (Fig. 3), which may confirm the photo-induced nature of the catalytic process.

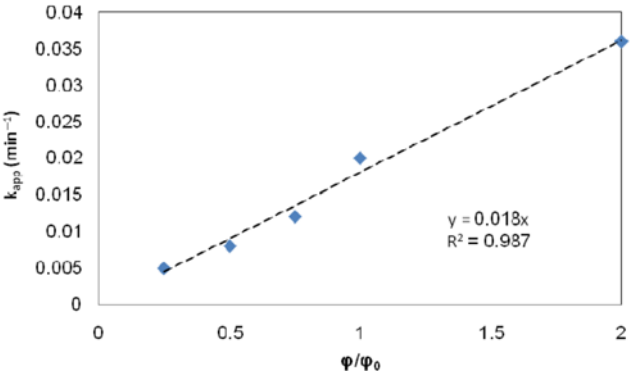

Fig. 3. Initial reaction rates as a function of light intensity.

3. Optimization of the Process by Response Surface Methodology

3-1. RSM Regression Equation and Model Analysis

CCD was employed to study the interactions between the significant factors and to determine their optimal levels. The design matrix of tested variables and the experimental data are given in Table 5. Multiple regression was used to analyze the data, the outcome of which was a second-order polynomial equation as follows:

$$\begin{aligned}\text{Phenol Degradation} = {} & +0.80 - 0.10 * X1 + 0.081 * X2 + 0.030 * X3 \\ & + 4.941E\text{-}003 * X4 + 0.015 * X1 * X2 \\ & - 0.018 * X1 * X3 + 4.809E\text{-}004 * X1 * X4 \\ & + 0.045 * X2 * X3 - 2.484E\text{-}003 * X2 * X4 \\ & - 4.684E\text{-}003 * X3 * X4 + 0.014 * X1^2 \\ & - 0.042 * X2^2 - 0.045 * X3^2 + 4.166E\text{-}003 * X4^2 \quad (2)\end{aligned}$$

The adequacy of the model was checked using ANOVA, as shown in Table 6. The "F-value" and the value of "Prob>F" for model were 6.83 and 0.003, respectively. These values may demonstrate the significance of the model. Among linear terms, parameters X_1 and

Table 5. Design matrix of experiments

Std	Run	Type	X1	X2	X3	X4	Phenol degradation
			Phenol con.	Catalyst loading	pH	Slurry flow rate	After 30 min
3	1	Fact	−1	+1	−1	−1	0.8251
8	2	Fact	+1	+1	+1	−1	0.7501
9	3	Fact	−1	−1	−1	+1	0.8599
13	4	Fact	−1	−1	+1	+1	0.8152
18	5	Axial	+2	0	0	0	0.6225
2	6	Fact	+1	−1	−1	−1	0.6128
15	7	Fact	−1	+1	+1	+1	0.9794
20	8	Axial	0	+2	0	0	0.8452
27	9	Center	0	0	0	0	0.8041
23	10	Axial	0	0	0	−2	0.7804
4	11	Fact	+1	+1	−1	−1	0.6878
6	12	Fact	+1	−1	+1	−1	0.5152
7	13	Fact	−1	+1	+1	−1	0.9764
28	14	Center	0	0	0	0	0.8123
16	15	Fact	+1	+1	+1	+1	0.7626
5	16	Fact	−1	−1	+1	−1	0.8021
10	17	Fact	+1	−1	−1	+1	0.6649
14	18	Fact	+1	−1	+1	+1	0.5287
21	19	Axial	0	0	−2	0	0.4138
19	20	Axial	0	−2	0	0	0.3263
12	21	Fact	+1	+1	−1	+1	0.6931
30	22	Center	0	0	0	0	0.7815
25	23	Center	0	0	0	0	0.8090
24	24	Axial	0	0	0	+2	0.7601
17	25	Axial	−2	0	0	0	0.9991
1	26	Fact	−1	−1	−1	−1	0.8393
11	27	Fact	−1	+1	−1	+1	0.8641
22	28	Axial	0	0	+2	0	0.7342
29	29	Center	0	0	0	0	0.8082
26	30	Center	0	0	0	0	0.8098

Table 6. ANOVA for response surface quadratic model

Source	Sum of squares	df	Mean square	F-value	p-value Proby>F
Model	0.59	14	0.042	6.83	0.0003
X1	0.26	1	0.26	41.95	<0.0001
X2	0.16	1	0.16	25.23	0.0002
X3	0.022	1	0.022	3.52	0.0804
X4	5.860E-004	1	5.860E-004	0.094	0.7628
X1X2	3.706E-003	1	3.706E-003	0.60	0.4516
X1X3	5.134E-003	1	5.134E-003	0.83	0.3774
X1X4	3.700E-006	1	3.700E-006	5.963E-004	0.9808
X2X3	0.032	1	0.032	5.14	0.0387
X2X4	9.872E-005	1	9.872E-005	0.016	0.9013
X3X4	3.510E-004	1	3.510E-004	0.057	0.8152
$X1^2$	5.612E-003	1	5.612E-003	0.90	0.3566
$X2^2$	0.048	1	0.048	7.78	0.0137
$X3^2$	0.055	1	0.055	8.91	0.0092
$X4^2$	4.762E-004	1	4.762E-004	0.077	0.7855
Residual	0.093	15	6.204E-003		

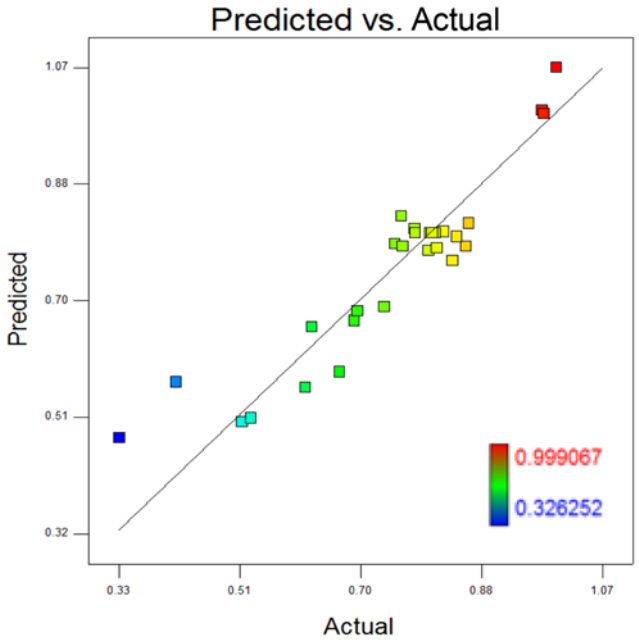

Fig. 4. Predicted vs. actual values for phenol degradation.

X_2, are always significant, while, X3, is rarely significant in phenol degradation. Similarly, among quadratic terms, $X2^2$, and $X3^2$, are both significant parameters in phenol degradation. Interactive term X2X3 is also significant in such a process. Regarding this conclusion, the model may be reduced to:

$$\text{Phenol Degradation} = +0.80 - 0.10 * X1 + 0.081 * X2 + 0.030 * X3 + 0.045 * X2 * X3 - 0.044 * X2^2 - 0.047 * X3^2 \quad (3)$$

In Fig. 4, predicted values for phenol degradation calculated from the reduced model have been plotted against those determined experimentally. The coefficient of determination (R^2) was calculated as 0.8901 for phenol degradation, indicating a good agreement between the experimental and the predicted data. The signal-to-noise ratio of 16.470 may be regarded as an adequate quantity. The coefficient of variation (CV) indicates the degree of reliability of the experimental procedure. The lower value for CV (9.17%) in this study is an indication of high reliability of the experiments performed. The "lack of fit p-value" of 0.1301 may imply that the lack of fit is not significant in comparison with the net error. In other words, there is only 13.01% chance that a large lack of fit F-value could occur due to noise. The model was found to be adequate for prediction within the range of variables employed.

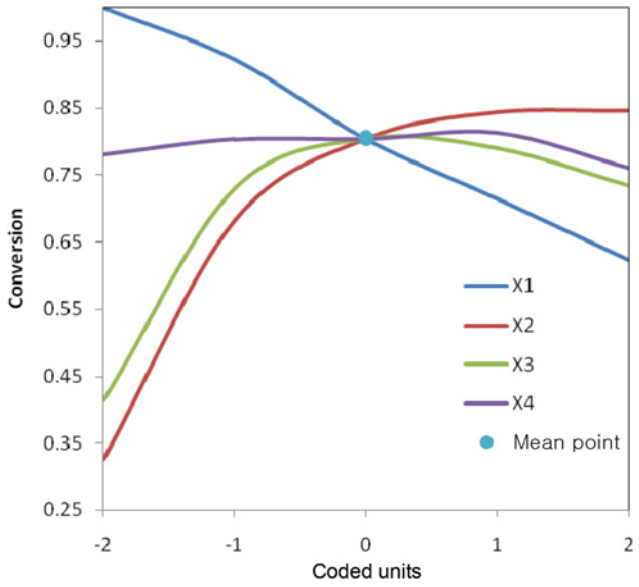

Fig. 5. Mean plot for tested factors.

3-2. Effect of the Significant Factors and Optimal Conditions

Mean plot of variables in Fig. 5 shows the effect of independent variables while holding the rest of variables at zero levels.

By increase in phenol concentration, higher amounts of reactant and reaction intermediates are adsorbed at the surface of the photocatalyst, thus reducing the generation of hydroxyl radicals due to the reduction in the number of active sites available for adsorption of hydroxyl anions. On the other hand, when phenol concentration is low, while the catalyst loading and light intensity remain unchanged, larger numbers of active sites and hydroxyl radicals are available to intermediates.

Adequate loading of the catalyst increases the generation rate of electron/hole pairs and thus, formation of •OH radicals, leading to the enhancement of photodegradation. Conversely, an excess amount of catalyst decreases the light penetration due to the shielding effect of the suspended particles [19,20] causing the reduction of photo degradation rate. In addition, such a rate reduction may be attributed to a screening effect due to the redundant dispersion of UV radiation as the result of substantial amount of suspended photocatalyst. Furthermore, under these conditions, particles tend to agglomerate, making a significant fraction of the catalyst to be inaccessible to either adsorbing the molecules or absorbing the radiation, with consequent decrease in the active sites available to the catalytic reaction.

The point of zero charge (pzc) of TiO_2 P25, i.e, the point when the surface charge density is zero, is reported to be between 6.2 and 6.8 [18,21]. The surface of the catalyst is positively charged at pH< pH_{pzc}, negatively charged at pH>pH_{pzc}, and remains neutral at pH= pH_{pzc}. These characteristics significantly affect not only the adsorption-desorption properties of TiO_2 surface, but also the changes of pollutant structure at various pH values. In aqueous media, phenol attains a pKa value of 9.9 (at 25 °C). This indicates that in solutions with pH<PKa, phenol is in the molecular form (C_6H_5OH). Whereas, at pH>PKa the phenol molecule undergoes deprotonation, becoming negatively charged ($C_6H_5O^-$) [19,21]. Thus, Electric charge properties of both, catalyst and substrate are found to play an important role in adsorption process, i.e., the interaction and affinity between both TiO_2 and phenol will vary with the solution pH. Thus, it may be concluded that an initial low acidic condition is suitable for effective phenol degradation.

The graphical representation of the regression model, known as the response surface plots, was determined using Design-Expert software and is presented in Fig. 6. In this figure, the effect of the two independent and significant variables on the process is demonstrated, while the rest of the variables have been kept at zero levels. In addition, a peak is clearly observable on the response surface, indicating that the optimum point is well inside the design boundary.

In Fig. 6, the effective interaction between pH and catalyst load-

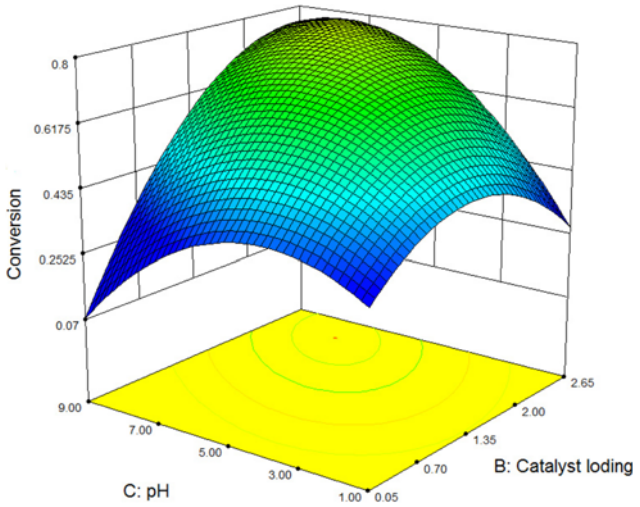

Fig. 6. Mutual interaction between the signiant factors.

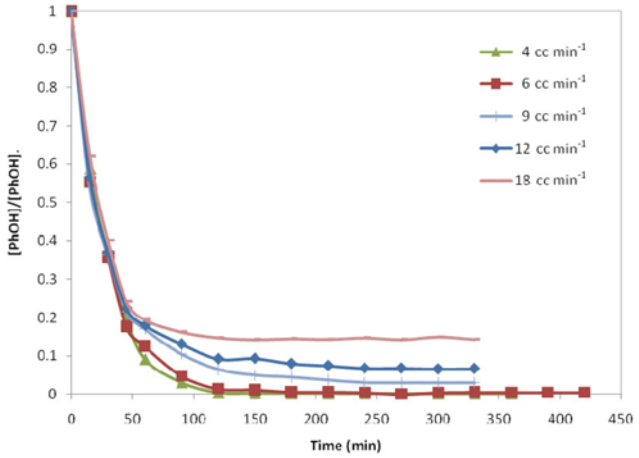

Fig. 7. Degradation of phenol by continuous flow photocatalytic treatment.

ing is demonstrated. Regarding that the PK_a value for the generation of hydroperoxyl radicals is 4.88,

$$^{\bullet}O_2^- + H^+ \leftrightarrow {}^{\bullet}OOH \qquad Pka=4.88 \tag{4}$$

Then, formation of such a radical is enhanced in acidic pH. On the other hand, in acidic solutions the tendency for agglomeration of the photocatalyst particles is rather high. Thus, in higher concentrations of photocatalyst the latter is quickly agglomerated and, as such, the ability of the photocatalyst in absorption of light and adsorption of pollutants at the catalyst surface are both declined, leading to the reduction in formation of positive electron-hole and oxidizing radicals. Owing to such effects, the rate of degradation reaction is reduced. In other words, at lower catalyst loading (corresponding to the low pollutant concentration) acidic pH is favorable, whereas at higher catalyst loading, the pH of the reaction media should be kept either neutral or very low acidic in order to prevent agglomeration of catalyst particles. In the latter case, however, the $^{\circ}OH$ formation is limited to the reaction between positive hole and water molecule or hydroxyl ion. In basic pH, formation of negative charges on TiO_2 surface reduces the pollutants adsorption onto catalyst surface and thus, lowers the rate of degradation.

Regarding the results derived from the statistically designed experiments, optimal conditions for degradation of 100 mg l^{-1} of phenol in water may be presented as follows, photocatalyst loading: 2.1 g l^{-1} pH 6.2 slurry flow rate: 550 ml min^{-1}.

3-3. Validation of the Model

The statistical model was validated by running test experiments using 100 mg l^{-1} of phenol, 2.1 g l^{-1} photo catalyst, pH 6.2 and 550 ml min^{-1} slurry flow rate. Under these optimized conditions, the predicted response for phenol degradation was 77.74% in 30 min, and the average of experimental values was 75.85% during the same time. As it is apparent, the experimental value was quite close to that predicted from the model, demonstrating the validity of the model.

4. Continuous Flow

Following optimization of the operating parameters, continuous photocatalytic treatment including TiO_2 separation and reuse of the latter was conducted (Fig. 1(b)). The reactor was first filled with water and loaded with 2.1 g l^{-1} of TiO_2. The circulation pump and UV lamps were then turned on. Ten minutes latter, continuous flow of feed (containing 100 mg l^{-1} of phenol) was introduced to the reactor. Discharge from the reactor was monitored with a flow rate identical to that of the feed.

The feed flow rates were set at 4, 6, 9, 12 and 18 ml min^{-1}, respectively. Fig. 7 shows the phenol concentration present in the treated solutions leaving the reactor. As it is expected, the degradation rate of phenol within the reactor is reduced by increase in feed flow rate. However, the results have shown a higher efficiency and an increased performance capability of the present reactor in comparison with the conventional processes carried out by Suryaman et al. [23]

An attempt was made to present a mathematical relation from which the continuous outlet phenol concentration could be determined. In this respect, a balance around the feed reservoir (Fig. 1(b)) was set up as follows,

$$Q_r C_{P_{r,out}} - Q_r C_{P_{r,in}} + vC_{P_{in}} - vC_{P_{out}} = 0 \tag{5}$$

where, v is the continuous volume flow rate of solution to the reservoir, $C_{P_{in}}$ and $C_{P_{out}}$ are the phenol concentration in the system inlet and outlet, Q_r is the volume flow rate of feed to the reactor, $C_{P_{r,in}}$ and $C_{P_{r,out}}$, are the phenol concentration in the reactor inlet and outlet. Values for $C_{P_{r,out}}$ may be determined from the following equation:

$$C_{P_{r,out}} = \int_0^{\infty} (C_P)_b E dt = \sum_i (C_P)_b E_i \Delta t_i \tag{6}$$

where, E is the residence time distribution function.

Assuming a pseudo-first-order kinetics for phenol decomposition [24] then,

$$C_{P_{r,out}} = C_{P_{r,in}} \sum_i e^{-k_{app}\Delta t\, i} E_i \Delta t \tag{7}$$

Hence,

$$D_{P_{out}} = \frac{vC_{P_{in}}}{v + Q_r(1 - \sum_i e^{-k_{app}\Delta t\, i} E_i \Delta t)} \tag{8}$$

According to the latter equation, in order to calculate the outlet concentration, the values for k_{app} at the steady state conditions and the residence time distribution of fluid in the reactor are both needed.

Table 7. Kinetic data from reference 24

$C_{P\ initial}$ (mg l^{-1})	$C_{P\ final}$ (mg l^{-1})	$C_{P\ average}$ (mg l^{-1})	k_{app} (min^{-1})
100	4.1	51.55	0.4566
75	0.13	37.56	0.5705
50	0	25	0.9437

Table 8. The experimental and predicted conversions in continuous system outlet

Q_r (ml min^{-1})	$X_{P\ out,\ exp.}$ (mg l^{-1})	$X_{P\ out,\ pre.}$ (mg l^{-1})
4	0.998	0.993
6	0.995	0.989
9	0.969	0.983
12	0.933	0.976
18	0.856	0.867

These data have been presented recently by Royaee et al. [24]. According to the kinetic data given in Table 7, k_{app} is inversely proportional to the phenol concentration. Furthermore, a correlation may be given for k_{app} as follows:

$$k_{app} = \frac{24.18}{C_P^{ave.}} - 0.036 \quad (min^{-1}) \tag{9}$$

To estimate the continuous outlet phenol concentration, Eqs. (8) and (9) should be solved simultaneously. In Table 8 the experimental and predicted conversions are both presented.

CONCLUSION

Continuous degradation of phenol has been studied using a photo-impinging streams reactor. Statistical experimental designs were first applied to optimize phenol degradation conditions carried out in the photoreactor. The results indicated that the statistical optimum strategy was an effective tool for optimization of process parameters of phenol degradation and for improving degradation efficiency. Optimal operating conditions determined in this study may be regarded as a solid foundation for further application of photo-impinging streams reactors in treatment of effluents containing phenol. The present investigation demonstrated the excellent ability of the photo-impinging streams reactors in decomposing a highly resistant compound (phenol).

REFERENCES

1. S. Ahmed, M. G. Rasul, R. Brown and M. A. Hashib, *J. Environ. Manage*., **92**, 311 (2011).
2. S. Shamaila, A. Khan Leghari Sajjad, F. Chen and J. Zhang, *Mater. Res. Bull*., **45**, 1375 (2010).
3. L. Laokiat, P. Khemthong, N. Grisdanurak, P. Sreearunothai, W. Pattanasiriwisawa and W. Klysubun, *Korean J. Chem. Eng*., **29**, 377 (2012).
4. J. H. Park, Y.-S. Seo, H.-S. Kim and I.-K. Kim, *Korean. J. Chem. Eng*., **28**, 1693 (2011).
5. M. Subramanian and A. Kannan, *Chem. Eng. Sci*., **65**, 2727 (2010).
6. D. Vildozo, C. Ferronato, M. Sleiman and J. M. Chovelon, *Appl. Catal. B: Environ*., **94**, 303 (2010).
7. T. Van Gerven, G. Mulc, J. Moulijn and A. Stankiewicz, *Chem. Eng. Process*., **46**, 781 (2007).
8. S. J. Royaee and M. Sohrabi, *Desalination*, **253**, 57 (2010).
9. S. J. Royaee, M. Sohrabi and F. Soleymani, *J. Chem. Technol. Biotechnol*., **86**, 205 (2011).
10. S. Meshram, R. Limaye, S. Ghodke, S. Nigam, S. Sonawane and R. Chikateb, *Chem. Eng. J*., **172**, 1008 (2011).
11. I. Hyoung Cho and K. Duk Zoh, *Dyes Pigm.*, **75**, 533 (2007).
12. D. Vildozo, C. Ferronato, M. Sleiman and J. M. Chovelon, *Appl. Catal. B: Environ*., **94**, 303 (2010).
13. Y. R. Abdel-Fattah, H. M. Saeed, Y. M. Gohar, M. A. El-Baz, *Process Biochnol*., **40**, 1707 (2005).
14. R. Gheshlaghi, J. M. Scharer, M. Moo-Young and P. L. Douglas, *Biotechnol. Bioeng*., **90**, 754 (2005).
15. P. F. Stanbury, A. Whitaker and S. J. Hall, *Media for industrial fermentations, In: Principles of Fermentation Technology*, Pergamon Press, Oxford, 93 (1986).
16. A. I. Khuri and J. A. Cornell, *Response surfaces: designs and analysis*, New York, Marcel Dekker, ASQA Quality Press (1996).
17. D. C. Montgomery, *Design and Analysis of Experiments*, 5th Ed. New York, John Wiley and Sons, 170 (2001).
18. D. F. Ollis, E. Pelizzetti and N. Serpone, *Environ. Sci. Technol*., **25**, 1523 (1991).
19. C. H. Chiou, C. Y. Wu and R. S. Juang, *Chem. Eng. J*., **139**, 322 (2008).
20. A. Sobczynski, L. Duczmal and W. Zmudzinski, *J. Mol. Catal. A: Chem*., **213**, 225 (2004).
21. K. Pujara, S. P. Kamble and V. G. Pangarkar, *Ind. Eng. Chem. Res*., **46**, 4257 (2007).
22. S. Malato, J. Blanco, C. Richter, B. Braun and M. I. Maldonado, *Appl. Catal. B: Environ*., **17**, 347 (1998).
23. D. Suryaman, K. Hasegawa, S. Kagaya and T. Yoshimura, *J. Hazard. Mater.*, **171**, 318 (2009).
24. S. J. Royaee and M. Sohrabi, *Ind. Eng. Chem. Res*., **51**, 4152 (2012).